Materials Transactions, Vol. 47, No. 1 (2006) pp. 239 to 242

RAPID PUBLICATION

Friction Stir Welding of Ultrafine Grained Interstitial Free Steels

Hidetoshi Fujii[1], Rintaro Ueji[2], Yutaka Takada[1], Hiromoto Kitahara[3], Nobuhiro Tsuji[3], Kazuhiro Nakata[1] and Kiyoshi Nogi[1]

[1]*Joining and Welding Research Institute, Osaka University, Ibaraki 567-0047, Japan*
[2]*Department of Advanced Materials Science, Kagawa University, Takamatsu 761-0396, Japan*
[3]*Department of Adaptive Machine Systems, Osaka University, Suita 565-0871, Japan*

Friction stir welding (FSW) was applied to ultra low-carbon interstitial free steels with mean grain sizes ranging from 0.7 μm, prepared by accumulative roll-bonding, to 27 μm. The steel with the intermediate grain size (1.8 μm) is most preferable for obtaining the highest hardness in the stir zone with the smallest grain size.

(Received November 14, 2005; Accepted November 28, 2005; Published January 15, 2006)

Keywords: *friction stir welding, accumulative roll bonding, steel, ultrafine grained microstructure*

1. Introduction

It has been well clarified, nowadays, that the high strengthened metallic materials with an ultrafine grained microstructure whose mean grain size is around or below 1 μm can be fabricated by severe plastic deformation (SPD) processes[1,2] such as accumulative roll-bonding (ARB),[2–4] and equal channel angular processing (ECAP).[5–7] For example, the ARB processed ultra low-carbon interstitial-free (IF) steel has an ultrafine grained microstructure with a grain size of 210 nm and high tensile strength of 819 MPa.[4] However, it is also clarified that the ultrafine grained microstructure with a single phase shows small elongation,[4] which provides the motivation to conduct post annealing aimed to recover the balance between the strength and ductility of the SPD processed materials. Some studies of the annealing phenomena clarified the normal (or continuous) grain growth[4,7] and abnormally low activation energy of the grain growth.[6]

In addition to the mechanical properties, the welding of the ultrafine grained materials are also important for structural use. If fusion welding is applied to ultrafine grained materials, grain growth easily occurs and the strength decreases. On the other hand, friction stir welding (FSW) can inhibit the grain growth because a lower heat is input during the FSW.[8–12] Thus, FSW should be a better welding method for ultrafine grained metals than fusion welding.

FSW has been mainly used for aluminum alloys because high melting temperature materials such as steel are difficult for FSW. However, steel is the most commonly used structural material. The aim of this study is to clarify the change in the mechanical properties and the microstructures by the FSW in the ultrafine grained steels fabricated by SPD. An annealed steel with the intermediate size between the ultrafine and conventional grain size are also studied to clarify the effect of the initial grain size on the mechanical properties of the FSW joints.

2. Experimental

Ultra low-carbon IF steel (20 ppm-C) was used in this study. The dimensions of the rectangular samples were 1.6 mm thick, 300 mm long and 30 mm wide. The ARB process was applied to the samples to obtain an ultrafine grained microstructure. The roll bonding of the process was conducted by a 50% reduction in one pass which was repeated 5 times. In order to obtain a sufficient bonding strength, the samples were heated in a furnace at 500°C for 10 min before each pass. After the roll bonding, the samples were cooled immediately in water. Some of the ARB samples were subsequently annealed at 600°C for 1.8 ks.

Three kinds of samples (the as-received, the as-ARB processed, and the annealed samples) were butt-welded along the rolling direction (RD) using an FSW machine. The tool, which was made of WC, had a 12 mm shoulder diameter, 4 mm probe diameter and 1.4 mm probe length. The tool was tilted by 3°. The rotation speed and the traveling speed were 400 min^{-1} and 400 mm/min, respectively. Ar shielding gas was used during the FSW. The temperature of the bottom surface at the weld center of the sample was measured using thermocouple during the welding.

The microstructures were characterized by optical microscopy, transmission electron microscopy (TEM) and electron back-scattering diffraction (EBSD) technique. Thin foils perpendicular to the transverse direction (TD) and parallel to the welding direction were cut from the center of the weld and electro-polished in a 100 mL HCO_4 + 900 mL CH_3COOH solution for the TEM observations. A Hitachi H-800 microscope was operated by 200 kV. The EBSD measurements were carried out using a program developed by TSL Inc. (OIM™) using a Philips XL30S SEM equipped with field emission operated at 20 kV. The planes parallel to the TD were cut from the weld and scanned by EBSD. A Vickers hardness test was conducted along the TD to evaluate the hardness profiles of the center of the thickness.

3. Results and Discussion

Figure 1 shows a color map indicating the crystallographic orientations of the as-received (a), the ARB processed (b) and the annealed samples (c). These color maps were obtained by EBSD measurements and the horizontal and the vertical directions in this figure are parallel to the TD and nominal direction (ND), respectively. The colors determined in the

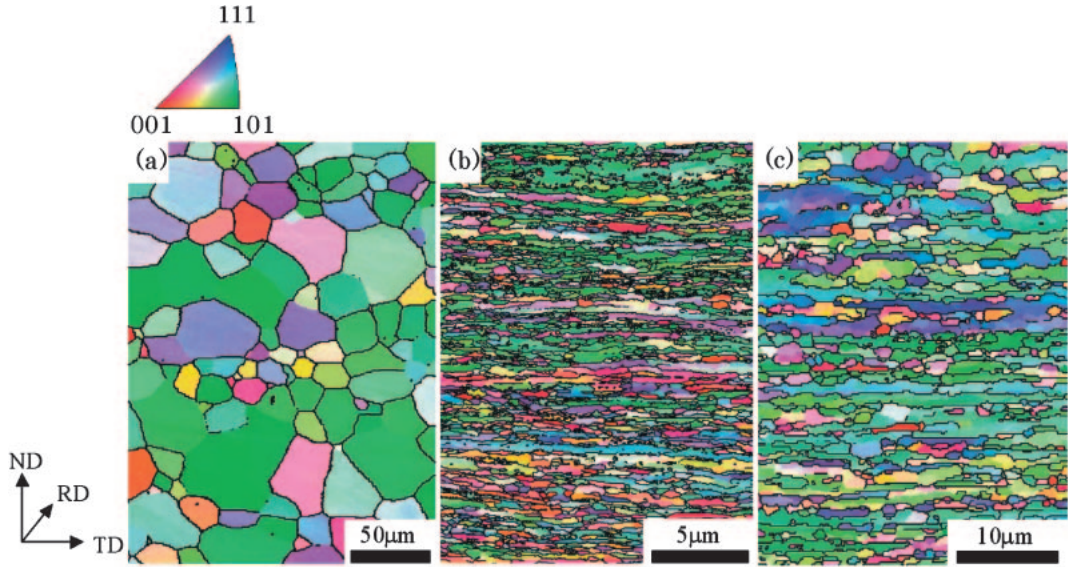

Fig. 1 OIM of IF steel base material obtained by EBSP measurement. (a) As received (b) ARB processed (c) Annealed steels.

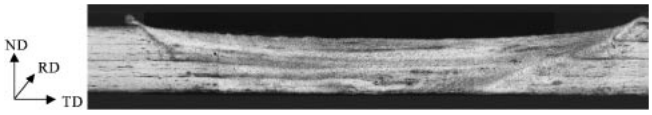

Fig. 2 Optical micrograph of transverse section of weld zone of ARB processed steel.

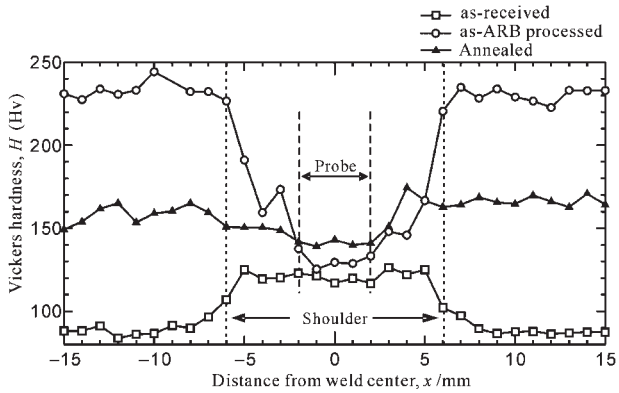

Fig. 3 Hardness profile of steel joints welded.

stereographic triangle indicate the crystallographic orientation parallel to the RD. The black lines are high-angle boundaries with misorientations higher than 15°. The as-received sample (a) shows the equiaxed grains whose mean grain size is 24.2 μm. The ARB processed samples shows a lamellar structure elongated parallel to the TD. The mean spacings of the high-angle boundaries along the ND and TD are 0.3 and 1.6 μm, respectively and the mean grain size is 0.7 μm. During the annealing of the as-ARB samples, grain growth takes place and the shape of the grain becomes somewhat equiaxed but still keeps its elongated feature. The mean grain size of the annealed sample is 1.8 μm.

Figure 2 shows an optical micrograph of the transverse section of the ARB processed steel joint. The welding center shows high degree of continuity and no defects. The temperatures of the bottom surfaces of the samples were around 650°C at the maximum during FSW, which is much lower than the α/γ transformation temperature (around 910°C).

The hardness profiles along the TD of the samples after FSW are shown in Fig. 3. The mean hardness of the base metals of the as-received, the ARB processed and the annealed samples are 91, 222, and 163 Hv, respectively, indicating that the hardness increases with the decreasing mean grain size. The hardness of the as-received and the ARB processed samples are changed in the stir zone. The hardness of the stir zone in the as-received sample increases to 120 Hv, whereas that in the as-ARB processed samples decreases to about 125 Hv. The stir zone in the ARB processed sample is slightly harder than that in the as-received. On the other hand, concerning the annealed sample, the hardness of the stir zone is slightly decreased, however, it still maintains a high hardness around 150 Hv. It should be noted that the stir zone in the annealed sample shows a higher hardness than those of the other two samples.

The RD orientation color maps at the center in thickness of the stir zone in the three samples are shown in Fig. 4. The green color showing the [011] // RD orientation is dominant in both the as-received and the as-ARB processed samples, while the mixture of many colors are detected, indicating the existence of various orientations in the stir zone of the annealed samples. In all three samples, the color changes inside some grains surrounded by black lines, indicating the existence of subgrains and/or dislocations. The mean grain sizes surrounded by high-angle boundaries in the stir zone of the as-received, the ARB processed and the annealed samples are 5.3, 3.1, and 2.0 μm, respectively.

Figure 5 shows the TEM bright field images of the stir zones in the as-received (a), the as-ARB processed (b) and the annealed (c) samples. The microstructures of all three samples consist of equiaxed grains including dislocations. The dislocation density seems to be higher than that in the stir

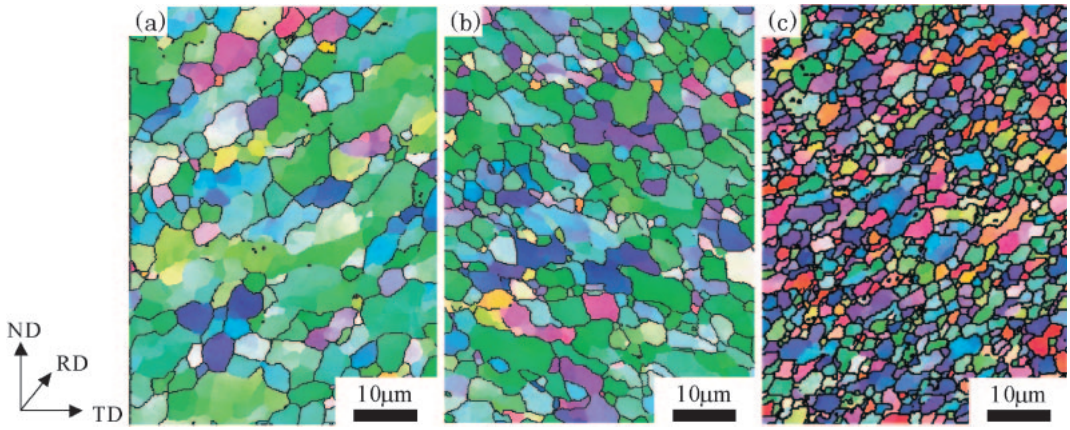

Fig. 4 OIM of stir zone obtained by EBSP measurement. (a) As received (b) ARB processed (c) Annealed steels.

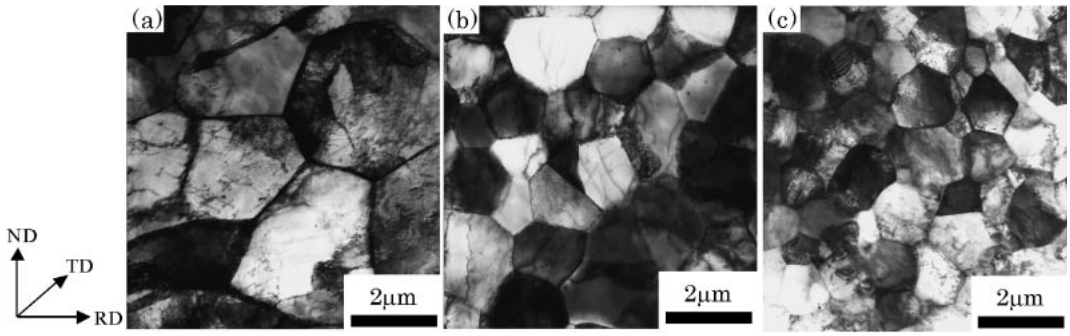

Fig. 5 TEM bright field images of stir zone. (a) As received (b) ARB processed (c) Annealed steels.

Table 1 Mean grain size and hardness of base metal and stir zone of steels.

	Base metal		Stir zone		
	Grain size (EBSD), d_{Base}/μm	Hardness, H_{Base}/Hv	Grain size (EBSD), $d_{stir,EBSD}$/μm	Grain size (TEM), $d_{stir,TEM}$/μm	Hardness, H_{stir}/Hv
As-received	24.2	91	5.3	2.4	120
As-ARB processed	0.7	222	3.1	1.1	125
Annealed	1.8	163	2.0	0.9	150

zone in the FSW processed commercial purity aluminium reported in a previous study.[12] This is caused by the restricted recovery during the FSW process due to the lower maximum temperature (650°C) reached by FSW, compared with the melting temperature of the steel (1530°C). The mean grain size, observed in the TEM images of the as-received, the as-ARB processed and the annealed samples are 2.4, 1.1 and 0.9 μm, respectively. All these values are smaller than those obtained by the EBSD measurements. These determinations of the smaller grain size by TEM are probably due to the existence of the low-angle grain boundaries in the stir zone for all the samples, although the difference in the observation (or measurement) direction between the TEM and EBSD is another possible reason. Anyhow, it can be clarified by both TEM observations and EBSD measurements that the hardness in the stir zone is higher with the decreasing (sub)grain sizes.

The grain size and hardness data were summarized in Table 1. The most important finding of the above experiments is that the annealed sample with the intermediate grain size (or intermediate hardness) in the base metal have the highest hardness in the stir zone after the FSW. It has been clarified that FSW gives rise to a large plastic flow in stir zone, which causes the introduction of many dislocations and the grain subdivision[13] by the dislocation boundaries to evolve fine grained microstructure. The dislocations and fine grains contribute to the strengthening of the stir zone. On the other hand, the heat generation by the plastic deformation provides the driving force of the recovery; the annihilation of the dislocation and the subgrain growth, resulting in decreasing the hardness. Generally, the generated heat is corresponding well to the plastic deformation energy which is the integration of the flow stress and strain. It is predictable that the flow stress of the as-ARB processed sample is the highest and the largest heat is then generated to enhance the recovery during the FSW process in this study. On the other

hand, in the as-received sample with a lower flow stress, the heat generation is smaller and the stir zone is then strengthened. However, the hardness of the base metal is smallest of the three so that the hardness in the stir zone becomes smaller than those of the as-ARB and the annealed samples. Consequently, the intermediate hardness in the base metal is preferable for obtaining a high hardness in the stir zone, due to the balance between the strengthening by the plastic flow and the recovery. However, the work hardening behaviors should be different between the steels with conventional grain size and ultrafine gains,[4] which makes it difficult to estimate the flow stress. In addition, although the geometric conditions are the same as shown in this study, the difference in the flow stress could cause the difference in the plastic flow behavior. Furthermore, the difference in the dislocation density between the deformed and the annealed states is another possible reason to inhibit the grain growth during FSW. These should be further studied to clarify the solid and logical relationships between the hardness of the stir zone and the base metal.

4. Summary

The hardness and microstructure of the FS welded IF steels with ultrafine grained microstructures fabricated by the ARB process were investigated. Also, the effect of the initial grain size on the strength of the FSW joint was clarified. The important results of this study can be summarized as follows:

(1) A 5-cycles ARB process decreases the mean grain size of the IF steel from 24.2 (as-received) to 0.7 μm. The grain size of the sample subsequently annealed at 600°C for 1.8 ks is 1.8 μm.

(2) The grain size of the stir zone is significantly affected by the initial grain size of the samples. The mean grain size in stir zone becomes smaller in order of the annealed sample, the ARB processed sample, and the as-received sample. The hardness of the stir zone increases with the decreasing mean grain size of the stir zone.

(3) The steel with an intermediate grain size (1.8 μm) is the most preferable to obtain the highest hardness in the stir zone with a small grain size.

Acknowledgment

The authors wish to acknowledge the financial support of the Toray Science Foundation, the Three Research Institute Project “Development Base of Joining Technology for New Metallic Glasses and Inorganic Materials,” “Priority Assistance of the Formation of Worldwide Renowned Centers of Research—The 21st Century COE Program (Project: Center of Excellence for Advanced Structural and Functional Materials Design)” from the Ministry of Education, Culture, Sports, Science and Technology of Japan, and a Grant-in-Aid for Science Research from Japan Society for Promotion of Science.

REFERENCES

1) T. C. Lowe and Y. T. Zhu: Adv. Eng. Mater. **5** (2003) 373–378.
2) N. Tsuji, Y. Saito, S. H. Lee and Y. Minamino: Adv. Eng. Mater. **5** (2003) 338–344.
3) Y. Saito, H. Utsunomiya, N. Tsuji and T. Sakai: Acta Mater. **47** (1999) 579–583.
4) N. Tsuji, Y. Ito, Y. Saito and Y. Minamino: Scr. Mater. **47** (2002) 893–899.
5) Y. Iwahashi, Z. Horita, M. Nemoto and T. G. Landon: Acta Mater. **45** (1997) 4733–4741.
6) M. Furukawa, Z. Horita, M. Nemoto, R. Valiev and T. G. Langdon: Acta Mater. **44** (1996) 4619–4629.
7) F. J. Humphreys, P. B. Prangnell, J. R. Bowen, A. Gholinia and C. Harris: Philos. Trans. R. Soc. London **357** (1999) 1663–1681.
8) H. J. Liu, M. Maeda, H. Fujii and K. Nogi: J. Mater. Sci. Lett. **22** (2003) 41–43.
9) H. J. Liu, H. Fujii, M. Maeda and K. Nogi: J. Mater. Proc. Technol. **142** (2003) 692–696.
10) W. B. Lee and S. B. Jung: Mater. Lett. **58** (2004) 1041–1046.
11) S. H. C. Park, Y. S. Sato, H. Kokawa, K. Okamoto, S. Hirano and M. Inagaki: Scr. Mater. **49** (2003) 1175–1180.
12) Y. S. Sato, Y. Kurihara, S. H. C. Park, H. Kokawa and N. Tsuji: Scr. Mater. **50** (2004) 57–60.
13) N. Hansen, X. Huang and D. A. Hughes: Mater. Sci. Eng. A **317** (2001) 3–11.